



## Receptive fields for smooth pursuit eye movements and motion perception

Kurt Debono<sup>a,\*</sup>, Alexander C. Schütz<sup>a</sup>, Miriam Spring<sup>a,b</sup>, Karl R. Gegenfurtner<sup>a</sup>

<sup>a</sup>Abteilung Allgemeine Psychologie, Justus-Liebig-Universität, Otto-Behaghel-Str. 10F, 35394 Giessen, Germany

<sup>b</sup>Department of Psychology & Center for Neural Science, New York University, NY, USA

### ARTICLE INFO

#### Article history:

Received 18 June 2010

Received in revised form 28 September 2010

#### Keywords:

Smooth pursuit  
Motion perception  
Random-dot kinematogram  
Motion integration  
Motion segmentation  
Motion perturbation  
Oculometric function  
Psychometric function

### ABSTRACT

Humans use smooth pursuit eye movements to track moving objects of interest. In order to track an object accurately, motion signals from the target have to be integrated and segmented from motion signals in the visual context. Most studies on pursuit eye movements used small visual targets against a featureless background, disregarding the requirements of our natural visual environment. Here, we tested the ability of the pursuit and the perceptual system to integrate motion signals across larger areas of the visual field. Stimuli were random-dot kinematograms containing a horizontal motion signal, which was perturbed by a spatially localized, peripheral motion signal. Perturbations appeared in a gaze-contingent coordinate system and had a different direction than the main motion including a vertical component. We measured pursuit and perceptual direction discrimination decisions and found that both steady-state pursuit and perception were influenced most by perturbation angles close to that of the main motion signal and only in regions close to the center of gaze. The narrow direction bandwidth (26 angular degrees full width at half height) and small spatial extent (8 degrees of visual angle standard deviation) correspond closely to tuning parameters of neurons in the middle temporal area (MT).

© 2010 Elsevier Ltd. All rights reserved.

### 1. Introduction

Smooth pursuit eye movements have for the most part been studied using small (<1 degree of visual angle (DVA)) foveal targets against a uniform featureless background (e.g. Rashbass, 1961). This approach underestimates the abilities of the pursuit system to: (a) integrate motion signals in order to follow large field targets and (b) isolate and follow some motion signals while ignoring others. Integration and segmentation processes have received more attention in recent literature. For instance, several studies have investigated the influence of additional motion signals on pursuit as well as perception (for a review see: Spring & Gegenfurtner (2008)), and some show that peripheral motion can modulate perception and pursuit in different ways (e.g. Spring & Gegenfurtner, 2007a).

Earlier studies used clearly distinct pursuit targets with different motion signals, such as multiple moving objects (e.g. Ferrera & Lisberger, 1997; Lisberger & Ferrera, 1997; Spring, Gegenfurtner, & Kerzel, 2006), a moving object and an independently-moving context (Miura, Kobayashi, & Kawano, 2009; Spring & Gegenfurtner, 2007a, 2007b), or a small target moving in front of a large-field background (e.g. Kodaka, Miura, Suehiro, Takemura, & Kawano, 2004; Lindner, Schwarz, & Ilg, 2001; Masson, Proteau, & Mestre, 1995). On the other hand, only a handful of studies measured spatial integration of pursuit eye movements to uniform, but spatially extended targets.

Heinen and Watamaniuk (1998) used coherently-moving random-dot kinematograms (RDK) at a fixed width of 10 DVA and showed that increasing RDK aperture height from 0.5 DVA to 10 DVA increases pursuit acceleration and decreases pursuit latency. When different motion vectors across a large field in a RDK do not share the same direction, but are distributed across a narrow bandwidth of directions, those vectors with similar directions are integrated for pursuit (Watamaniuk & Heinen, 1999), and perception (Watamaniuk, Sekuler, & Williams, 1989).

In the present study we asked two questions: (1) How does the pursuit system treat multiple motion vectors that are presented in different spatial locations across the visual field? (2) Are pursuit and perception equally sensitive to extrafoveal motion signals? The ultimate goal of this study was to map a receptive field for smooth pursuit eye movements, which we are calling an 'oculoceptive field', akin to receptive fields for visual neurons. We asked observers to pursue the large-field coherent motion signal inside a RDK. The coherent signal could be perturbed by shifting some of the dots in a direction offset obliquely from that of the signal, thus creating a secondary extrafoveal motion signal throughout pursuit. The perturbations were presented in several gaze-contingent regions around gaze position. We measured the effects of the direction of perturbations, and also the effects of the spatial size and position of the perturbation regions relative to gaze, on the direction of the pursuit response. In all five experiments presented here, we also asked observers to report perceived motion direction after each trial so that we could compare pursuit response to the perceived direction. We used the perceptual

\* Corresponding author. Fax: +49 641 99 26 119.

E-mail address: [kurt.debono@psychol.uni-giessen.de](mailto:kurt.debono@psychol.uni-giessen.de) (K. Debono).

responses to map a ‘perceptive field’, which we compared to the oculocceptive field.

## 2. Methods

### 2.1. Overview of experiments

We conducted five experiments to map an oculocceptive field for pursuit, and a perceptive field for perception. We did this by presenting coherently moving dots (masked by noise) as a signal for pursuing while perturbing regions around the gaze position by changing the direction of a percentage of dots in the region. Observers were instructed to pursue the motion signal and to indicate at the end of each trial whether they perceived the overall motion direction to be up or down relative to horizontal motion.

#### 2.1.1. Experiment 1: Oculometric and psychometric functions without perturbation

To determine the effect of signal angle on direction discrimination, we used a range of signal angles (0 angular degrees ( $^{\circ}$ ),  $\pm 2^{\circ}$ ,  $\pm 5^{\circ}$ ,  $\pm 10^{\circ}$ ). The  $0^{\circ}$  (horizontal) signal angle condition served as a baseline for oculometric analysis.

#### 2.1.2. Experiment 2: Oculometric and psychometric functions with a $10^{\circ}$ perturbation

We compared the effect of perturbation angles  $\pm 10^{\circ}$  on pursued and perceived signal direction. Perturbation trials had signal angles of  $0^{\circ}$ ,  $\pm 2^{\circ}$ ,  $\pm 5^{\circ}$  or  $\pm 10^{\circ}$  with a perturbed region in front of the gaze position. We included unperturbed trials at a signal angle of  $0^{\circ}$  as a baseline.

#### 2.1.3. Experiment 3: Varying the perturbation angle

To measure the effect of the perturbation angle, unperturbed trials with signal angles  $0^{\circ}$  and  $\pm 5^{\circ}$  were randomly interleaved with perturbation trials with signal angles  $0^{\circ}$  or  $\pm 5^{\circ}$  and perturbation angles  $\pm 5^{\circ}$ ,  $\pm 10^{\circ}$ ,  $\pm 15^{\circ}$ ,  $\pm 20^{\circ}$ ,  $\pm 25^{\circ}$ ,  $\pm 45^{\circ}$ , or  $\pm 90^{\circ}$ . Perturbations for this experiment were located in front of the gaze position. The mean within each signal angle group served as a baseline (same for experiments 4 and 5).

#### 2.1.4. Experiment 4: Varying the perturbation location

To test the effect of perturbation location, perturbation trials (signal angles  $0^{\circ}$  or  $\pm 5^{\circ}$ , perturbation angles  $\pm 10^{\circ}$ ) had a perturbation region that was presented above, below, in front of, or behind the gaze position. Perturbation trials were randomly interleaved with unperturbed trials at signal angles  $0^{\circ}$  or  $\pm 5^{\circ}$ .

#### 2.1.5. Experiment 5: Varying the perturbation width and eccentricity

We varied the width and eccentricity of the perturbation region to quantify the extent of spatial integration of motion information for pursuit and perception. Perturbation trials (signal angle  $0^{\circ}$ , perturbation angles  $\pm 10^{\circ}$ ) were randomly interleaved with unperturbed trials (signal angles  $0^{\circ}$ ,  $\pm 2^{\circ}$ , or  $\pm 5^{\circ}$ ). Only perturbation trials and signal-only trials with a  $0^{\circ}$  signal angle were analyzed in this experiment.

### 2.2. Observers

Participants were ten trained observers, seven females and three males (mean age  $24 \pm 4$  yrs). Not all observers took part in all experiments: 10 participants took part in experiment 1, 8 in experiment 2, 7 in experiment 3, 8 in experiment 4, and 8 in experiment 5. For each condition, observers did 112, 72 and 960 trials for experiments 1–3 respectively. For experiment 4, observers did 360 trials for the condition with a perturbation, and 720 trials for the

condition without a perturbation. For experiment 5, observers did between 80 and 120 trials per condition. The variability in number of trials across experiments resulted from the way we later collapsed some of the conditions, since conditions reported here represent the grouped conditions shown in the figures of this study. Author K.D. participated in all experiments; all other observers were unaware of the purpose of the study. All observers had normal or corrected-to-normal visual acuity.

### 2.3. Equipment

Observers were seated in a dimly-illuminated room, with their head stabilized by a chin rest and a forehead support, in front of a 19" Sony Trinitron F520 CRT monitor,  $40 \times 31$  cm ( $1280 \times 1024$  pixel resolution, 100 Hz refresh rate), driven by an Nvidia Quadro NVS 290 graphics board. The center of the monitor was at eye level and the viewing distance was 47 cm. The active screen area was circular, centered in the middle of the monitor, and subtended 40 DVA. Observers viewed the screen binocularly, while movements of the right eye were recorded at 2000 Hz (Eyelink 1000; SR Research Ltd., Mississauga, Ontario, Canada). We used standard procedures to calibrate the eye tracker and validate eye position. Stimulus display and data collection were controlled by a PC.

### 2.4. Visual stimuli

The central fixation spot was a bull’s-eye with an outer radius of 0.3 DVA and an inner radius of 0.15 DVA. The stimulus was a RDK that had white dots with a luminance of  $87 \text{ cd/m}^2$  moving at 10 DVA/s and a limited lifetime of 200 ms, presented on a black background with a luminance of  $0.04 \text{ cd/m}^2$ . When expired, each dot reappeared at a random position within the aperture for subsequent 200-ms lifetimes, so that the overall dot density of the aperture was kept constant at 2 dots/DVA. The phase of each dot’s lifetime cycles was shifted randomly to prevent all dots from being relocated at the same time. The RDK consisted of 20% signal dots, moving coherently in a common direction across lifetimes, thereby giving the impression of global motion across the aperture and providing a signal for pursuit. The remaining 80% of the dots were noise dots with a random initial direction of displacement every subsequent lifetime. The direction distribution of the noise dots at each lifetime was isotropic. Signal motion was rightward or leftward along the horizontal meridian or offset obliquely upwards or downwards from the horizontal in steps of  $2^{\circ}$ ,  $5^{\circ}$ , and  $10^{\circ}$ . We decided to use a 20:80 signal-to-noise ratio since our own pilot studies indicated that observers reach close to 100% accuracy with a higher signal-to-noise ratio (data not presented here).

To perturb a region of the stimulus, 20% of the signal dots and 20% of the noise dots inside that region were turned into perturbation dots. Perturbation dots had the same characteristics as signal dots, but differed in motion direction. They moved obliquely upwards or downwards but in the same left/right general direction of (or, in the case of a  $90^{\circ}$  perturbation, perpendicular to) signal motion. For experiments 2–4, perturbations were presented in one of four regions inside a circular window around gaze position. The window was composed of two concentric circles (centered on the gaze position) with an inner-circle radius of 2 DVA and an outer-circle radius of 10 DVA. The resulting ring-shaped area between these two circles was divided into four regions: above, below, to the right, or left of gaze position. The four regions had borders along the crossing diagonals of the circular window, and were equal in size and shape (Fig. 1C). The borders of the perturbation regions were not visible to the observers. The regions were gaze-contingent and reacted to an eye movement with a latency of  $<10$  ms. In experiment 5, perturbations were presented inside a gaze-contingent rectangular region of varying width (2–10 DVA)

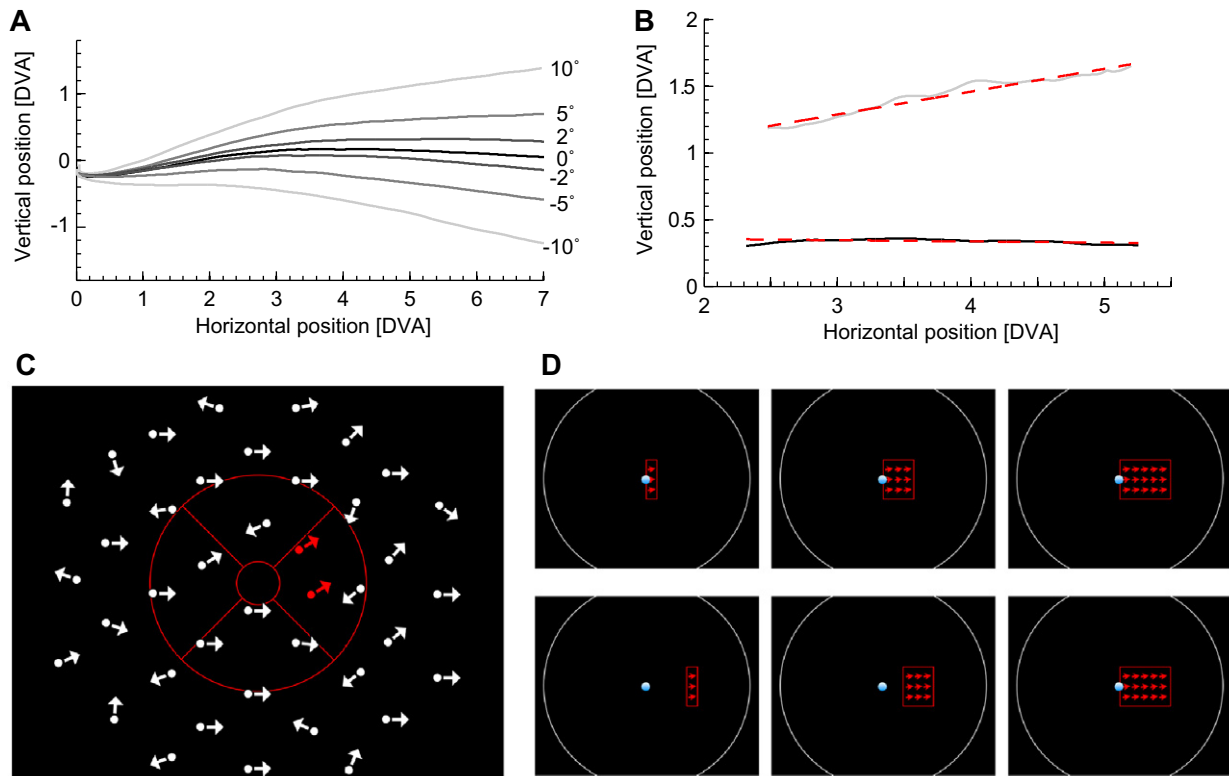


**Fig. 1.** Experimental paradigm and analysis of pursuit decisions. (A) Averaged eye position traces of a representative observer (S.K.) during pursuit of coherent motion at various signal angles (numbers on the right). (B) Eye position traces of a representative observer (S.K.) during a 300 ms time interval centered on 700 ms after stimulus presentation. The horizontal black line represents the mean eye trace for a rightward horizontal signal (0 baseline angle). The grey line represents a single eye trace following an upward 10° signal. Each trace is fit with a robust multilinear regression line (red dashed lines) representing the estimated direction of the eye during the time window. (C) Cartoon of a perturbation trial in which an upward perturbation (red arrows) is presented in front of the gaze position (inner concentric circle) together with a rightward-moving horizontal signal (rightward-pointing white arrows) embedded in noise. Red lines represent the gaze-contingent coordinate system. Arrows and lines are shown for illustration purposes only. (D) Different perturbation regions in experiment 5. Blue dots represent gaze position, red rectangle and red arrows represent the perturbation regions and direction of perturbation when signal is moving rightward (0°). The upper row shows perturbation regions expanding from the gaze position outwards, the lower row shows perturbation regions expanding inwards.

and a fixed height of 8 DVA. Perturbation regions were presented either in front of, or behind the gaze position and could either expand from 10 DVA towards the gaze position (inwards) or expand away from the gaze position towards 10 DVA (outwards), in steps of 2–10 DVA (Fig. 1D). The perturbation region was always centered vertically on the stimulus midline but was shifted horizontally to the right (when signal was rightward) or to the left (when signal was leftward) of the gaze position, starting from the gaze position.

### 2.5. Experimental procedure

Observers were instructed to pursue the coherent motion of the stimulus in each trial. Each trial started with a fixation spot in the center of the screen and observers initiated stimulus motion by pressing a button while fixating the spot. Stimulus motion duration was 1000 ms. At the end of each trial they indicated whether signal motion was upwards or downwards relative to horizontal motion by pressing the 'up' or 'down' arrow keys on the keyboard.

### 2.6. Psychometric analysis

We obtained psychometric functions representing the proportion of perceptual upward decisions as a function of signal angle. Observers' responses to leftward and rightward stimuli were symmetrical and were grouped. We fitted cumulative Gaussian functions to this data and estimated the point of subjective equality (PSE) and the standard deviation (SD) using the Psignifit toolbox in Matlab (Wichmann & Hill, 2001). A perceptual decision ceiling

effect was reached for oblique signal angles by all observers in experiments 3–5, so only perceptual decisions for trials with a horizontal signal angle were analyzed.

### 2.7. Eye movement analysis

Recorded eye position traces were stored on disk and analyzed off-line using Matlab (MathWorks, Inc., Natick, MA). We used the standard EyeLink saccade detection algorithm with a combined velocity (22°/s) and acceleration criterion (8000°/s<sup>2</sup>). We filtered eye-position signals using a Butterworth filter with a cut-off frequency of 30 Hz. To analyze the direction of each eye trace, we fitted a robust multilinear regression line to each vertical vs. horizontal eye-position trace (Fig. 1A and B) at various time windows throughout a trial. Traces containing saccades during the analysis window or blinks during the stimulus duration (5.4%) were excluded from analysis. In the following sections,  $A_s$  represents the angle of this regression line for each eye trace recorded during presentation of a signal-only trial, and  $A_p$  represents the angle of the regression line for each eye trace recorded during presentation of a perturbation trial.

### 2.8. Oculometric analysis

Eye traces for each observer were grouped according to signal angle and general direction of signal (leftwards vs. rightwards), then compared to a baseline. For experiments 1 and 2, the mean  $A_s$  for 0° signal condition was used as the baseline, while for

experiments 3–5, the baseline was the mean  $A_s$  within each signal angle group. The difference between each  $A_s$  (experiment 1) or each  $A_p$  (experiments 2–5) and its respective baseline (see above: Overview of experiments) was calculated. Angular data were converted to binary decisions by classifying eye traces (during specified time windows) with angular directions above their respective baseline as ‘upward’ decisions and those below the baseline as ‘downward’ decisions by the eye. Observers’ response profiles to leftward and rightward stimuli were symmetrical and were grouped. In order to compare binary eye movement decisions to psychophysical judgments, we computed oculometric functions using the same procedure described above for psychometric functions. The SDs of the resulting oculometric functions represented their steepness. Steeper functions (ones with smaller SDs) indicated more precise position information available to the visuomotor system during pursuit. We compared the SDs of the oculometric functions for different time windows to the single SD of the psychometric function (which did not vary over time for each trial) in order to find a time window with the closest

match between oculometric and psychometric data (Fig. 2A). A time interval of 300 ms, centered on 700 ms after stimulus presentation was the earliest time window that represented the closest stable match between oculometric and psychometric data and thus yielded the highest measured precision. We did not choose a 500 ms-long time window as this would not have shown fine changes in pursuit direction throughout the window. Moreover, we did not choose a very late time window due to possible anticipatory slowing towards the end of the trial (Kowler & Steinman, 1979a, 1979b). The chosen window was used as the default time window for oculometric analyses in experiments 2, 4 and 5.

### 3. Results

#### 3.1. Experiment 1: Oculometric and psychometric functions without perturbation

For 10 observers, we varied the signal angle without perturbation to obtain baseline oculometric and psychometric functions. Fig. 2C

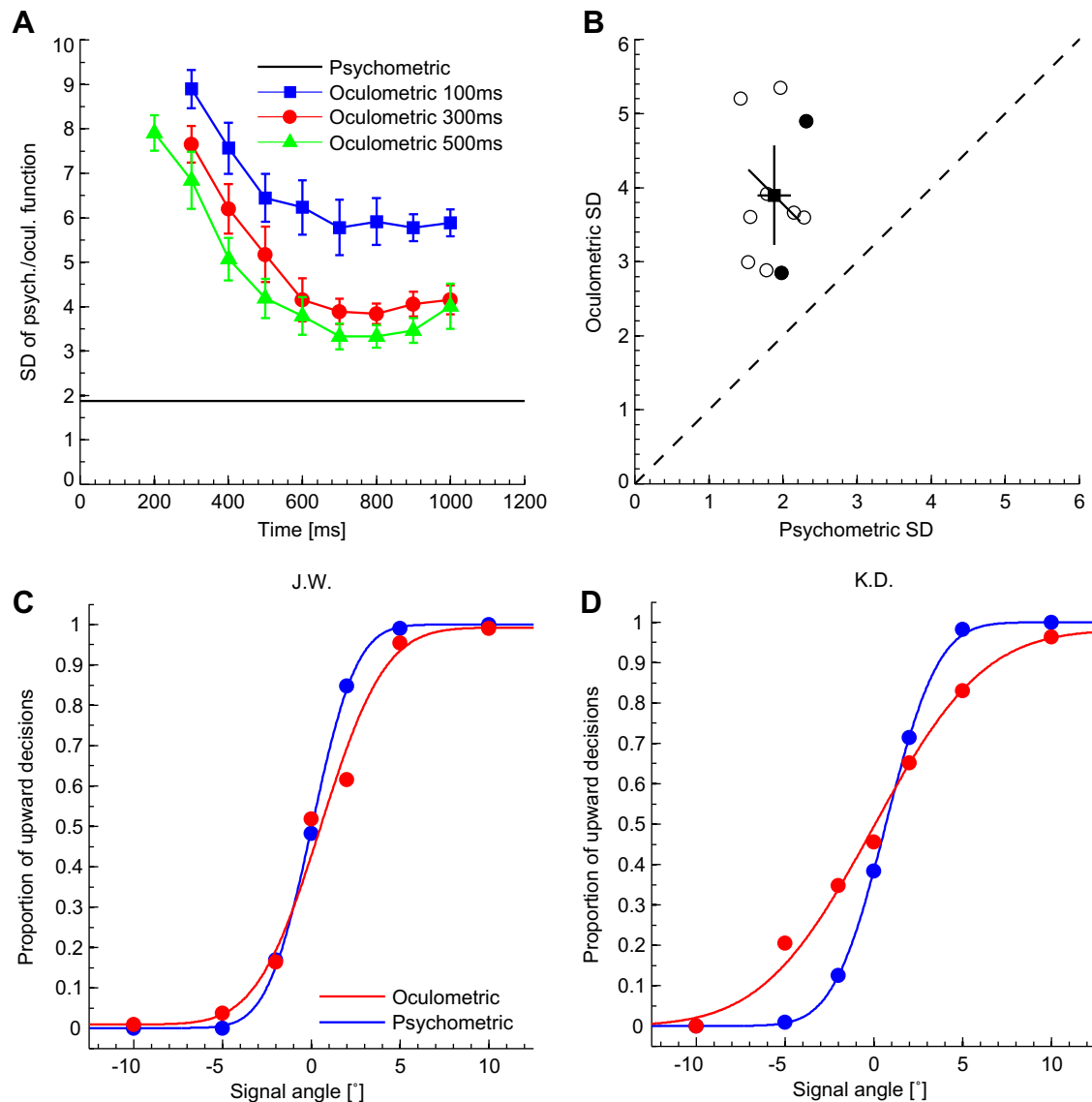


**Fig. 2.** Oculometric and psychometric functions without perturbation. (A) SDs of psychometric and oculometric functions averaged across all observers. Error bars represent standard errors. Different colors indicate different time windows for eye movement analysis. The black horizontal line indicates the SD of the psychometric function. (B) SDs of oculometric (estimated from a 300 ms time interval centered at 700 ms) and psychometric functions for 10 observers (circles) and their mean (filled square). Error bars represent 95% C.I. Filled circles represent the two representative observers in panels C and D. (C–D) Comparison of oculometric (red) and psychometric (blue) functions for two representative observers (J.W. & K.D.).

and D shows the comparison between oculometric (red) and psychometric (blue) functions for two representative observers. While the PSEs were similar for oculometric and psychometric functions for both observers, the SDs differed: the slopes of the psychometric functions were steeper than those of the oculometric functions.

Across observers, the average PSE was  $0.13^\circ$  ( $SD = 0.4$ ) for the oculometric functions and  $0.31^\circ$  ( $SD = 1.5$ ) for the psychometric functions. These values were not significantly different (paired  $t$ -test,  $t(9) = 6.5732$ ;  $p = 0.744$ ). The average SD was  $3.9$  ( $SD = 0.9$ ) for oculometric functions, and  $1.9$  ( $SD = 0.3$ ) for psychometric functions. This difference was significant (paired  $t$ -test( $9$ ) =  $6.5732$ ;  $p < 0.001$ ), indicating that perceptual decisions were more precise when compared to pursuit decisions (Fig. 2B).

### 3.2. Experiment 2: Oculometric and psychometric functions with a $10^\circ$ perturbation

In this experiment we investigated how psychometric and oculometric functions are affected by a  $10^\circ$  perturbation angle ( $n = 8$ ). Fig. 3A and B shows psychometric (blue) and oculometric functions

(red) comparing trials with an upward ( $+10^\circ$ ) perturbation to those with a downward ( $-10^\circ$ ) perturbation for two representative observers. A comparison of both oculometric and psychometric functions for upward and downward perturbations shows that the curves for upward perturbations are shifted leftwards for both observers, indicating that for all signal angles tested, the likelihood of an upward decision increased with an upward perturbation when compared to a downward perturbation. There was hardly any change in the steepness of the functions when the perturbation was upward when compared to downward, indicating that there was very little change in precision of information derived from the stimulus with the switch in perturbation direction. Psychometric functions were steeper than oculometric ones, which is similar to what we found in experiment 1.

The average oculometric PSE was  $0.99^\circ$  ( $SD = 0.5$ ) and  $-0.96^\circ$  ( $SD = 0.4$ ) for downward and upward perturbations respectively (Fig. 3C). The average psychometric PSE was  $1.37^\circ$  ( $SD = 1.7$ ) and  $-0.19^\circ$  ( $SD = 1.4$ ). To test these effects statistically, we calculated a repeated-measures ANOVA with factors function type (psychometric vs. oculometric) and perturbation direction (downward vs.

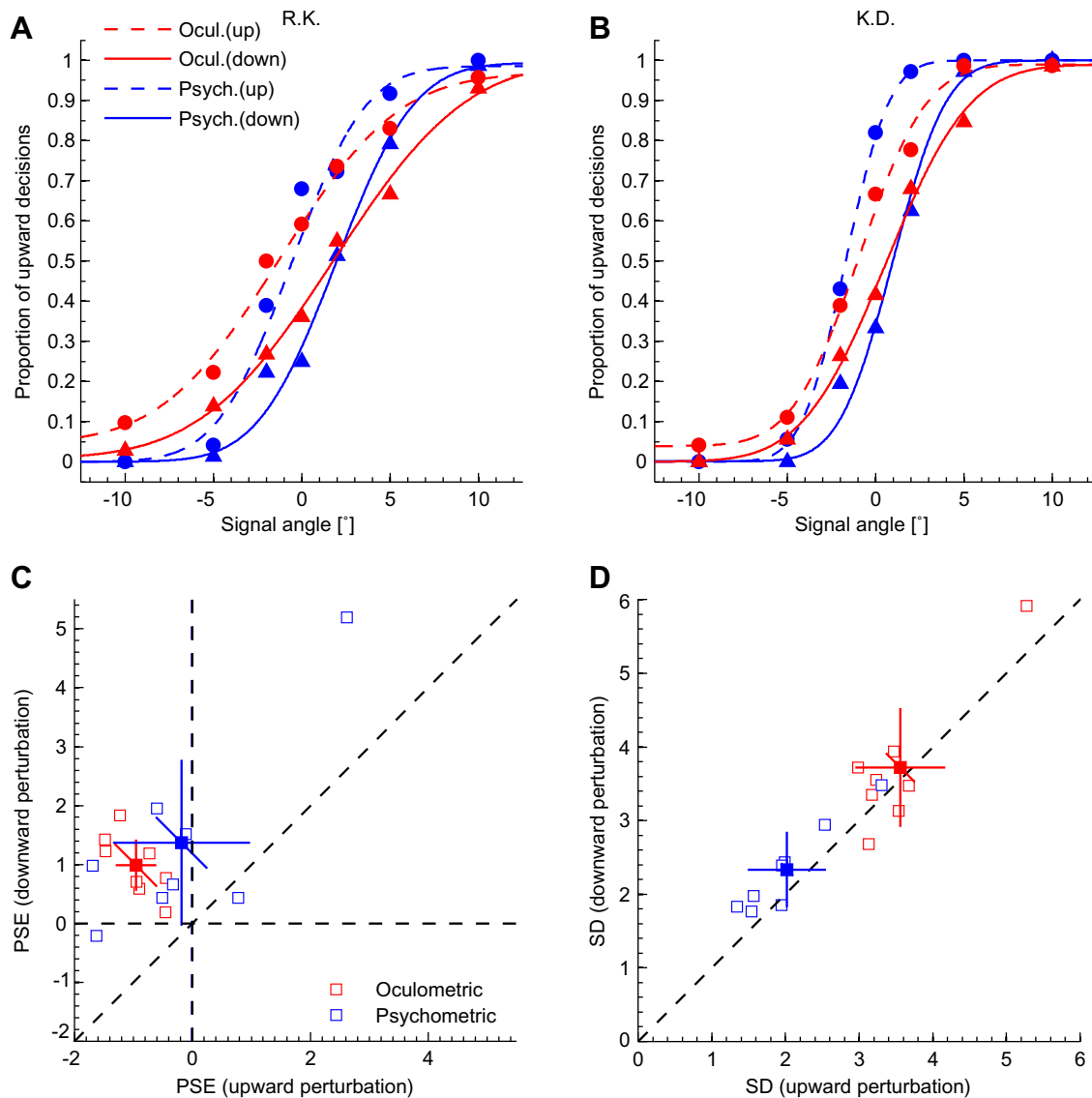


**Fig. 3.** Oculometric and psychometric functions with  $10^\circ$  perturbation. (A–B) Oculometric (red) and psychometric (blue) functions with a  $10^\circ$  upward (dashed lines and circles) and downward (solid lines and triangles) perturbation for two representative observers (R.K. & K.D.). PSEs (C) and SDs (D) of these oculometric and psychometric functions for all observers tested. Single observer data is plotted in open symbols; the averaged data across observers in filled symbols. Error bars represent 95% C.I.

upward). The main effect for function type was not significant ( $F(1, 7) = 1.315, p = 0.290$ ), but the main effect for perturbation direction was significant ( $F(1, 7) = 43.469, p < 0.01$ ). The two-way interaction was not significant ( $F(1, 7) = 0.886, p = 0.378$ ). These results indicate that the PSE for psychometric and oculometric functions were affected in the same way by the perturbation.

Results were quite different for the SD (Fig. 3D). The average oculometric SD was 3.7 ( $SD = 1.0$ ) for downward and 3.6 ( $SD = 0.7$ ) for upward perturbations. The same values for the psychometric SD were 2.3 ( $SD = 0.6$ ) and 2.0 ( $SD = 0.6$ ). We calculated a repeated-measures ANOVA with the factors function type (psychometric vs. oculometric) and perturbation direction (downward vs. upward). The main effect for function type was significant ( $F(1, 7) = 61.170, p < 0.01$ ), as was the main effect for perturbation direction ( $F(1, 7) = 8.118, p < 0.05$ ). The two-way interaction was not significant ( $F(1, 7) = 0.652, p = 0.446$ ). Experiment 2 therefore replicated the slope difference between the psychometric and oculometric functions that we observed in experiment 1.

### 3.3. Experiment 3: Perturbation angle

In this experiment we investigated how different perturbation angles ( $\pm 5^\circ, \pm 10^\circ, \pm 15^\circ, \pm 20^\circ, \pm 25^\circ, \pm 45^\circ$  and  $\pm 90^\circ$ ) affect perceptual and pursuit decisions ( $n = 7$ ). For each signal angle tested we computed the percentage of pursuit and perceptual up/down decisions that agreed with the up/down perturbation direction (Fig. 4A). The computed percentages for upward and downward perturbations and for signal angles ( $0^\circ, \pm 5^\circ$ ) were similar and therefore grouped for analysis. Data in blue show the mean pursuit decisions across subjects during an early time window (300 ms time interval centered on 300 ms after target motion onset). The percentage of decisions congruent with perturbation direction increased, peaked at a tested perturbation angle of  $25^\circ$  and declined to zero as the angle of perturbation was increased further. In contrast, for a later 300 ms time interval that was centered on 700 ms after motion onset (orange), the effect on pursuit peaked at  $10^\circ$ . For this later time window, as the angle of perturbation was increased to  $45^\circ$ , the effect not only declined, but became negative by deviating away from the perturbation. For perceptual responses, the percentage of decisions congruent with perturbation direction peaked at the smallest perturbation angle of  $5^\circ$  and declined sharply with larger

perturbation angles, becoming negative with a  $90^\circ$  perturbation angle. The relatively large error bars for perceptual responses indicate more perceptual variability between observers relative to their pursuit responses.

Converting the eye movements into a binary pursuit decision during an early and a late time window allowed us to compare pursuit decisions with perceptual ones, but on the other hand prevented us from looking at the rest of the pursuit response throughout the stimulus duration. In order to achieve a better temporal and spatial resolution, we analyzed average eye directions in various 300 ms time windows, thus covering a range from 150 to 950 ms after target motion onset. We wanted to obtain a perturbation direction tuning curve for pursuit with the premise that if all perturbation angles would be equally effective, the resulting raw eye directions would deviate systematically away from the signal direction as a function of increasing perturbation angle. As we were interested in the relative weighting of the different perturbation directions, we isolated this effect by dividing the raw eye direction by the sine of the perturbation angle, which yields an estimation of efficiency. A value of zero indicates that the eye does not follow the perturbation at all, while a value of unity indicates that the eye follows only the perturbation direction. The resulting tuning curves (Fig. 4B) show a broader direction tuning for early, rather than late time windows. These tuning curves show only half of the perturbation direction tuning, since we tested only perturbations in the same general left/right direction of the signal. Here we assumed the tuning curve to be roughly symmetric for perturbations moving in the same general direction of, and in a direction opposite to the signal, so that we simply multiplied the width of our curve by 2 in order to derive the full tuning curve width. The full width at half height (FWHH) of the tuning curve changed from  $62^\circ$  at a time window centered on 300 ms, to  $26^\circ$  at a time centered on 700 ms. This is interesting because it shows that direction tuning is not constant throughout the stimulus duration, and highlights the online flexibility of the pursuit system.

### 3.4. Experiment 4: Perturbation location

In experiments 2 and 3, the perturbation was presented in a region in front of the gaze position during pursuit (Fig. 1C). In experiment 4, we tested how a perturbation influences pursuit and

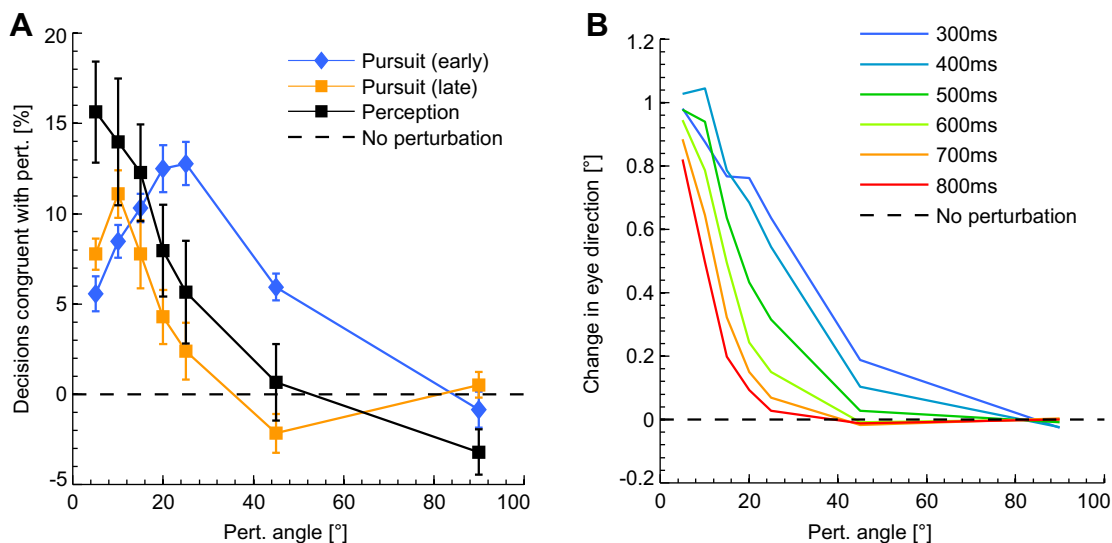


**Fig. 4.** Effect of perturbation angle. (A) The percentage of early and late pursuit and perceptual decisions that agree with the perturbation direction as a function of perturbation angle. The decision percentages are relative to those of the condition without perturbation (dashed line). (B) Change in eye direction for different time windows. The changes in eye direction are relative to those of the condition without perturbation (dashed line). Panels represent averaged data for 7 observers. Error bars represent standard errors.

perception when it is presented in different gaze-contingent regions ( $n = 8$ ). Therefore, during pursuit of a signal, subjects were presented with  $10^\circ$  perturbations inside one of the four regions around the gaze position, as described in Section 2. Again, we computed the percentage of pursuit and perceptual up/down decisions that agreed with the up/down perturbation direction.

As expected, perturbations presented in front of the gaze position had a stronger influence on perception than on pursuit. This replicates our results presented in experiment 3. This stronger influence on perception was also present for the other three regions around the gaze position (Fig. 5A). On average, for perception there was no effect difference between the regions in front (16.6%,  $SD = 12.9$ ), above (16.25%,  $SD = 6.1$ ) and below (17.2%,  $SD = 6.9$ ) the gaze position, while a relatively large effect was present for the perturbation region behind the gaze position (29.9%,  $SD = 5.3$ ). This means that perceptually, motion integration from a perturbation behind the gaze position was stronger compared to integration from the other three regions. Integration differences between the

four perturbation regions were milder for pursuit decisions, although the effects of the regions in front (10.4%,  $SD = 4.9$ ) and behind (11.1%,  $SD = 4.9$ ) were slightly larger than the effects of regions above (7.7%,  $SD = 1.9$ ) and below (5.5%,  $SD = 3.0$ ) the gaze position. This suggests that pursuit decisions were influenced more by perturbations presented in regions along the pursuit trajectory. Despite these trends in the averaged data, there were strong inter-individual differences in the relative pursuit and perceptual integration of different perturbation regions (Fig. 5B and C).

To test these effects statistically, we calculated a repeated-measures ANOVA with the factors perturbation position (front, behind, above, below) and judgment type (perceptual vs. pursuit). The main effect of position was significant ( $F(3, 21) = 9.200, p < 0.01$ ) suggesting that these effects were actually different at different perturbation regions. The main effect for judgment type was also significant ( $F(1, 7) = 20.547, p < 0.01$ ), indicating that the effects were larger for perception than for pursuit. The two-way interaction was significant ( $F(3, 21) = 11.545, p < 0.01$ ), thus highlighting

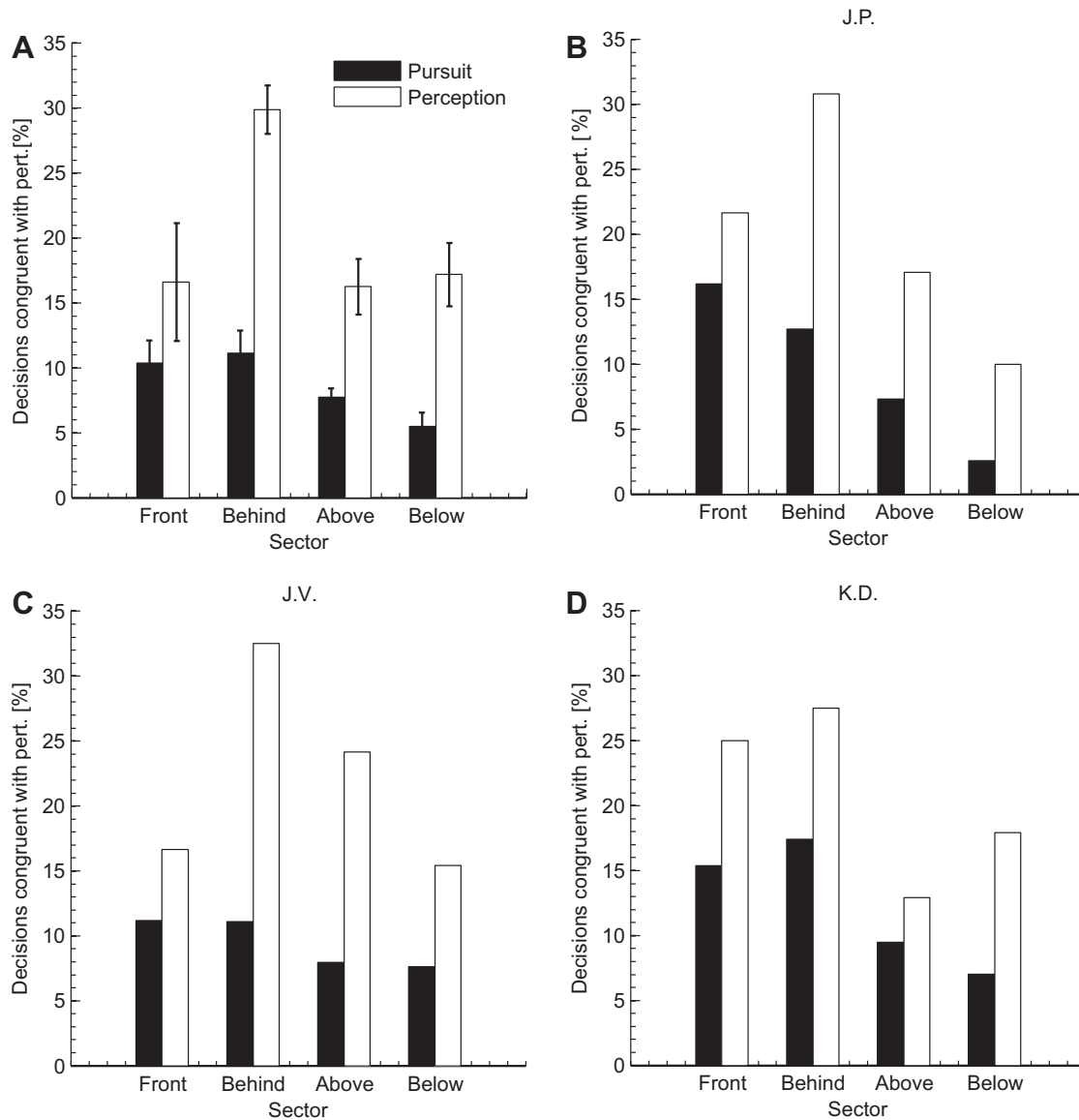


**Fig. 5.** Effects of perturbation location. Comparison of pursuit and perceptual decisions that agree with the perturbation direction for perturbations presented in front, behind, above and below gaze position during pursuit. The decision percentages are relative to those of the condition without perturbation. Panels represent averaged data for 8 observers (A) as well as three typical observers J.P., J.V. & K.D. (B, C, D respectively). Error bars represent standard errors.

the exceptionally large perceptual effect of a perturbation behind the gaze position during pursuit.

### 3.5. Experiment 5: Perturbation width and eccentricity

Experiments 2–4 measured the influence of a perturbation in regions of a fixed size and a fixed eccentricity away from gaze position. In experiment 5 we measured the influence of a perturbation in systematically-varied region sizes and eccentricities away from gaze position during pursuit ( $n = 8$ ).

We varied the width and eccentricity of the perturbation area along the horizontal meridian during horizontal pursuit. In one condition, we increased the area of the perturbation region in two-DVA steps outwards, away from the gaze position thus increasing eccentricity. In the other condition, we increased the area inwards from a 10 DVA eccentricity, towards the gaze position. Both conditions were tested either behind or in front of gaze position. Each step size was presented throughout a whole trial as a gaze-contingent perturbation region during pursuit. For each of the perturbation regions we calculated the percentage of perceptual and pursuit decisions congruent with the perturbation direction, as a raw measurement. Ultimately we strived to estimate the spatial profile of the oculoeceptive and perceptive fields. As we changed the perturbation area in different trials (either increasing the area, in inward or outward steps, or decreasing the area, in inward or outward steps), the influence of the perturbation region at each size/eccentricity was represented by the difference between neighboring raw measurements. Hence we first differentiated the raw measurements for all four conditions (inward vs. outward, front vs. back). As the differentiated values for inward and outward conditions represent the same measurement, we averaged across these conditions. We then fitted a cumulative Gaussian function to the differentiated data in order to estimate the spatial parameters of the oculoeceptive and perceptive fields.

As predicted by our previous experiments, perceptual integration effects were larger than pursuit ones, especially when the perturbation was presented behind the gaze position during pursuit. Fig. 6A and B shows the effect of a systematic horizontal expansion of the perturbation region outwards from gaze position on pursuit and perceptual decisions; Fig. 6C and D shows the effect on decisions as the perturbation region expanded horizontally inwards towards gaze position. In both conditions, the perturbation effect increased with increasing size of the perturbation area. Interestingly, the slopes of the functions were different when the perturbation area expanded outwards vs. inwards relative to gaze position: if the area expanded outwards, the function was negatively accelerated, indicating a lower influence for more eccentric positions; if the area expanded inwards, the function was positively accelerated, indicating a higher influence of positions closer to the gaze position. The functions in Fig. 6A–D were obtained by integrating the Gaussian fit from data in Fig. 6E (see below).

Based on these findings we constructed the spatial profile of the oculoeceptive and perceptive fields. In order to obtain the raw effect of the perturbation region at different eccentricities, we differentiated the decision percentages (calculated above) from each other. We averaged the differentiated values for the inward and outward expanding conditions because they represented the same measurement. We fitted a Gaussian function to these values to estimate the parameters of the oculoeceptive and perceptive fields (Fig. 6E). The oculoeceptive field was centered at 0 DVA and had a FWHH of 7.8 DVA. The perceptive field was shifted slightly backwards by 0.75 DVA and had a FWHH of 10.5 DVA. These results suggest that motion signals close to the gaze position were more strongly integrated for perception and pursuit than more eccentric motion signals. We also analyzed the oculoeceptive field at different time windows during pursuit (similar to the direction tuning analysis in experiment 3). Unlike the sharpening of the directional tuning with later time windows, the size and position of the

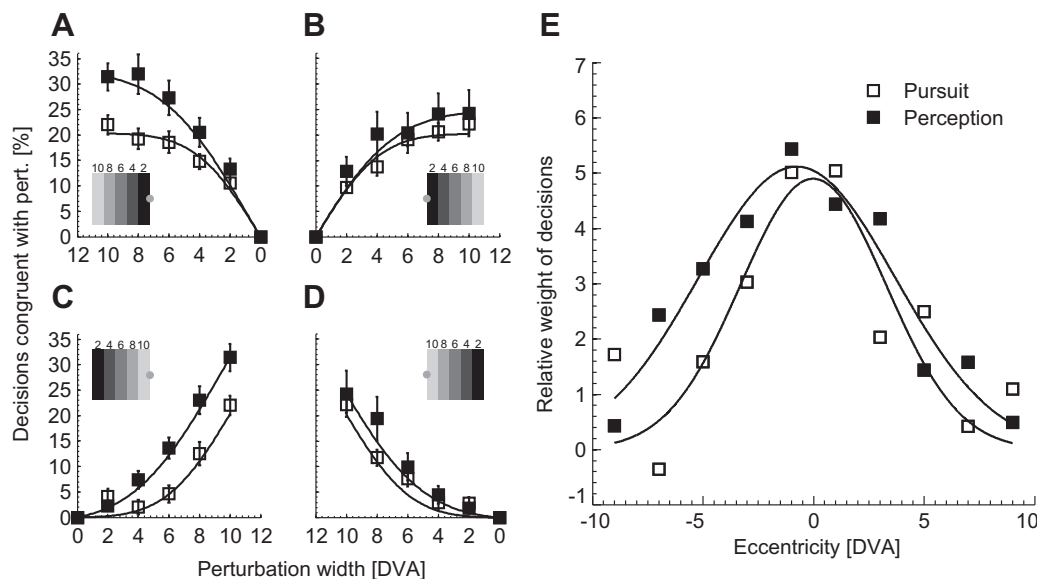


**Fig. 6.** Effects of perturbation width and eccentricity. (A–D) Pursuit and perceptual decisions that agree with the perturbation direction as a function of variations in width and eccentricity of the perturbation region. The decision percentages are relative to those of the condition without perturbation. B, D represent data for stimuli with a perturbation in front of the pursuit target while A, C represent data for stimuli with a perturbation behind the pursuit target. Inlays represent the outward stretch (A and B) or inward stretch (C and D) of the perturbation region. Symbols represent the average across subjects; error bars denote the standard error of the mean; lines are obtained by fitting a Gaussian function to the differentiated values in E. Numbers on the shaded diagrams represent the perturbation width. Shaded bars represent regions that were perturbed in different conditions with the darkest bar representing a region that was always presented with a perturbation and the lightest bar representing a perturbation region that was perturbed once during a perturbed signal condition. The bull's eye at the edge of the inlay represents the foveal position. (E) Receptive field profile for perception and pursuit. Negative numbers indicate perturbations behind the fovea and positive numbers indicate perturbations in front of the fovea. Symbols represent the average across subjects; lines are obtained by fitting a Gaussian function to the data.

perturbation did not change the oculomotor field profile in a systematic way over time.

#### 4. Discussion

In this study we aimed to map out an oculomotor field for the pursuit motion integration system and a perceptive field for perceptual motion integration. In general we showed that pursuit to a large field is sensitive to, and moves in the direction of weak localized changes in signal direction. Perception of motion direction during pursuit showed in general very similar direction sensitivity to that of pursuit. When we computed spatial receptive fields for pursuit and perception we found that the oculomotor field was centered on the gaze position whereas the perceptive field was shifted slightly behind the gaze position.

##### 4.1. Motion integration mechanisms

Motion integration studies have shown that the smooth pursuit system uses different mechanisms to cope with multiple vectors moving at the same time in the visual field. Masson and colleagues (Masson & Stone, 2002; Wallace, Stone, & Masson, 2005) used large (~12 DVA) line-figure objects with ambiguous local motion signals that were different from the object's veridical 2D motion direction. These shapes resemble real-world moving objects with multiple local edges and different orientations. With these objects as pursuit targets, eye movements are usually initiated in the direction of the vector average of the 1D motion signals and corrected towards the object's veridical motion direction after ~200 ms. A similar behavior has been found with single tilted lines in monkey eye movements (Pack & Born, 2001) and human direction and speed estimation (Castet, Lorenceau, Shiffrar, & Bonnet, 1993; Lorenceau, Shiffrar, Wells, & Castet, 1993).

Another type of object frequently used for the study of ocular tracking (in this case: short-latency ocular following) is a large (~25 DVA) moving plaid, composed of two superimposed gratings with different orientations and motion directions (Masson & Castet, 2002). When both gratings move in opposite directions (type I plaid), the earliest eye-movement response moves in the direction of the vector average of the two components. When one grating is moving while the other is stationary (unikinetic, or type II plaid), the temporal dynamics of the eye-movement response resembles findings obtained with line figures: movements are usually initiated in the direction of the moving grating (local motion) and in the object's veridical, global motion direction towards the end of the open-loop phase, after ~70–100 ms (Barthelemy, Fleuriot, & Masson, 2010; Masson & Castet, 2002). These findings are in agreement with neurophysiological results showing that pattern motion selectivity in macaque medial temporal area (MT) is delayed relative to component motion selectivity and builds up over ~100 ms (Pack, Berezovskii, & Born, 2001; Smith, Majaj, & Movshon, 2005). Hence, there is a close link between the initiation of smooth pursuit eye movements and the neural activity in area MT (Lisberger & Movshon, 1999).

The above studies show that motion information can be integrated across space by one of two mechanisms: (1) Vector averaging of the various directions (e.g. Groh, Born, & Newsome, 1997; Lisberger & Ferrera, 1997; Recanzone & Wurtz, 1999), yielding a global motion response; (2) Winner-take-all mechanisms, where one direction is chosen while other vectors are discarded (e.g. when there is a time delay between target and distractor: Ferrera & Lisberger, 1997; Recanzone & Wurtz, 1999), resulting in a local motion response. Taken together, these findings demonstrate that motion signals can be integrated over large areas of the visual field, and that ocular tracking responses can change dynamically over

time. However, in most cases these studies used stimuli with different motion signals that covered the foveal region as well as the extrafoveal space. Furthermore, they only measured eye movements, not perception, and focused mostly on the pursuit initiation phase.

In our study, small perturbation angles, when presented in a gaze-contingent region in front of the gaze position were integrated maximally by both steady-state pursuit and perception. Larger perturbation angles decreased this integrative effect of pursuit and perception as a function of increasing angle size, even though the vertical component of the perturbation vector was larger for larger perturbation angles. Interestingly, the directional tuning of early pursuit responses showed a broader bandwidth when compared to the tuning of later pursuit responses, essentially sharpening the bandwidth over time. During steady-state pursuit (around 700 ms after stimulus onset), the tuning bandwidth that we found (of approximately 26°) is consistent with the lowest bandwidth found in MT neurons (Albright, 1984). For 90° perturbations, pursuit gaze even deviated away from the perturbation direction. This is similar to what Spering and colleagues (2007a, 2006) found when observers were instructed to pursue a horizontally moving target while avoiding a second stimulus or context that appeared during steady-state pursuit and moved in a different direction. Pursuit deviated in the opposite direction to that of the distractor (Spering et al., 2006) or context perturbation (Spering & Gegenfurtner, 2007a), rather than integrating target and distractor.

##### 4.2. Spatial integration during pursuit

We found that a perturbation region influenced the eyes more when it was presented spatially close to the fovea and this effect declined gradually when the perturbation region was further away from the fovea in different trials. The FWHM of the oculomotor field (7.8 DVA) is again similar to the smallest receptive fields in MT neurons (Felleman & Kaas, 1984). Such a small oculomotor field makes sense because motion vectors in our natural visual environment are more likely to belong to the pursued target if they are physically closer to it and moving in a similar direction. However, it has also been shown that pursuit can integrate across a larger area (Heinen & Watamaniuk, 1998): if the size of a coherent motion field increases, pursuit latency decreases and pursuit acceleration increases.

##### 4.3. Comparing pursuit and perception

The directional tuning as well as the size of the receptive fields were similar for pursuit and perception. However, we also found a few striking differences. First, direction discrimination was better for perception than for pursuit (psychometric functions were steeper than oculometric functions). A similar difference between pursuit and perception has been reported in other direction discrimination studies, using a parallelogram (Beutter & Stone, 2000) or a plaid stimulus (Beutter & Stone, 1998). Interestingly, for speed discrimination, pursuit and perception seem to be similar (Gegenfurtner, Xing, Scott, & Hawken, 2003).

Second, pursuit and perception were influenced differently by the four spatial positions of the gaze-contingent perturbation sectors (experiment 4): pursuit was influenced more by perturbations presented along the pursuit trajectory when compared to the influence of those above or below the gaze position, while perception was influenced much more by perturbations behind the gaze position when compared to the influence of the other three sectors. These results are similar to those of experiment 5, where the perceptive field was found to be slightly shifted behind the gaze position by 0.75 DVA, rather than being centered on the gaze

position like the oculomotor field. Therefore we report perceptual asymmetries between integration of motion in the direction of pursuit and motion in the wake of pursuit. On the retina, the retinal slip of perturbations in front or behind the gaze position is the same, leading to an identical retinal input. The only remaining difference is the spatial position of the perturbation (in front or behind) relative to the gaze position during pursuit. Perceptual asymmetries of this sort could be caused by attention. Visual attention, as measured by an alphanumeric discrimination task during pursuit, has been shown to be located at the tracked target (Khurana & Kowler, 1987; Lovejoy, Fowler, & Krauzlis, 2009) with no apparent spatial bias. This indicates that spatial attention might be distributed symmetrically around the tracked target. On the other hand, some have claimed, based on reaction time asymmetries, that visual attention is located ahead of gaze position. Such studies found shorter reaction times, both saccadic (Blohm, Missal, & Lefevre, 2005; Kanai, van der Geest, & Frens, 2003; Smeets & Bekkering, 2000; Tanaka, Yoshida, & Fukushima, 1998), and manual (van Donkelaar & Drew, 2002), to a peripheral target flashed ahead of gaze position during pursuit. These results hint at a possible visual attention bias ahead of gaze position, in the direction of pursuit. However, shorter reaction times to flashed targets during pursuit might simply reflect the capacity of an abrupt onset to capture visual attention (Yantis & Jonides, 1984) rather than the spatial location of attention (Lovejoy, Fowler, & Krauzlis, 2009). Also, shorter reaction times are not an index of how accurate space is represented in front or behind the gaze position, and here, accuracy might be more relevant for our study. On the contrary, it seems that longer, rather than shorter reaction times of saccades elicited during pursuit are associated with more spatially accurate saccades, i.e. ones that take into account not only the retinal position error of the flashed target on the retina, but also the smooth eye displacement (Blohm et al., 2005). Therefore, the longer latency of saccades to flashed foveal targets during pursuit (targets flashed behind the gaze position) reported by some (e.g. Blohm et al., 2005) might reflect a more accurate representation of space behind the gaze position that could be relied upon more by the perceptual system. The issue is far from being resolved here, and it would be interesting to explore this perceptual asymmetry further, for instance by varying pursuit signal velocity or perturbation strength.

## 5. Conclusion

Our study describes motion integration mechanisms during pursuit. We can speculate why such mechanisms exist by looking at the properties of real-world moving objects that are usually pursued. The system might be taking into account the physics of motion to better predict the target's movement. For instance, when integrating motion vectors during pursuit, it might be taking into account the inertia of the target by assuming that if the vectors are moving along one trajectory they will likely keep moving in the same direction and will not make sharp direction changes. Thus the system could be tuned only to small shifts in the vectors in the vicinity of the gaze position, and weigh those vectors closest to the target more than those that are further away. By doing so, the system might better respond to gradual, rather than sudden changes in target direction by integrating motion vectors of a similar direction and close to the target. For optimal target selection, it also readily discards vectors moving in more eccentric locations, even though these could be moving in the same general direction. Such vectors are less likely to be part of the target. As far as we can tell, these pursuit properties seem to be an automatic response of the system and not associated with top-down information such as saliency.

## Acknowledgments

This work was supported by the EU Marie-Curie ITN “Co-ordination for Optimal Decisions in Dynamic Environments” and the DFG Forschergruppe FOR 560 “Perception and Action”. We thank Harold Bedell for helpful discussions and Sarah Jill Wagner for help with data collection.

## References

- Albright, T. (1984). Direction and orientation selectivity of neurons in visual area MT of the macaque. *Journal of Neurophysiology*, 52(6), 1106.
- Barthelemy, F. V., Fleuriot, J., & Masson, G. S. (2010). Temporal dynamics of 2D motion integration for ocular following in macaque monkeys. *Journal of Neurophysiology*, 103(3), 1275.
- Butter, B., & Stone, L. (1998). Human motion perception and smooth eye movements show similar directional biases for elongated apertures. *Vision Research*, 38(9), 1273–1286.
- Butter, B., & Stone, L. (2000). Motion coherence affects human perception and pursuit similarly. *Visual Neuroscience*, 17(01), 139–153.
- Blohm, G., Missal, M., & Lefevre, P. (2005). Processing of retinal and extraretinal signals for memory-guided saccades during smooth pursuit. *Journal of Neurophysiology*, 93(3), 1510–1522.
- Castet, E., Lorenceau, J., Shiffrar, M., & Bonnet, C. (1993). Perceived speed of moving lines depends on orientation, length, speed and luminance. *Vision Research*, 33(14), 1921–1936.
- Felleman, D., & Kaas, J. (1984). Receptive-field properties of neurons in middle temporal visual area (MT) of owl monkeys. *Journal of Neurophysiology*, 52(3), 488.
- Ferrera, V. P., & Lisberger, S. G. (1997). Neuronal responses in visual areas MT and MST during smooth pursuit target selection. *Journal of Neurophysiology*, 78(3), 1433.
- Gegenfurtner, K. R., Xing, D., Scott, B. H., & Hawken, M. J. (2003). A comparison of pursuit eye movement and perceptual performance in speed discrimination. *Journal of Vision*, 3(11), 865–876.
- Groh, J., Born, R., & Newsome, W. (1997). How is a sensory map read out? Effects of microstimulation in visual area MT on saccades and smooth pursuit eye movements. *Journal of Neuroscience*, 17(11), 4312.
- Heinen, S. J., & Watamaniuk, S. N. J. (1998). Spatial integration in human smooth pursuit. *Vision Research*, 38(23), 3785–3794.
- Kanai, R., van der Geest, J., & Frens, M. (2003). Inhibition of saccade initiation by preceding smooth pursuit. *Experimental Brain Research*, 148(3), 300–307.
- Khurana, B., & Kowler, E. (1987). Shared attentional control of smooth eye movement and perception. *Vision Research*, 27(9), 1603–1618.
- Kodaka, Y., Miura, K., Suehiro, K., Takemura, A., & Kawano, K. (2004). Ocular tracking of moving targets: Effects of perturbing the background. *Journal of Neurophysiology*, 91(6), 2474.
- Kowler, E., & Steinman, R. M. (1979a). The effect of expectations on slow oculomotor control. I. Periodic target steps. *Vision Research*, 19, 619–632.
- Kowler, E., & Steinman, R. M. (1979b). The effect of expectations on slow oculomotor control. II. Single target displacements. *Vision Research*, 19, 633–646.
- Lindner, A., Schwarz, U., & Ilg, U. (2001). Cancellation of self-induced retinal image motion during smooth pursuit eye movements. *Vision Research*, 41(13), 1685–1694.
- Lisberger, S. G., & Ferrera, V. P. (1997). Vector averaging for smooth pursuit eye movements initiated by two moving targets in monkeys. *Journal of Neuroscience*, 17(19), 7490.
- Lisberger, S. G., & Movshon, J. A. (1999). Visual motion analysis for pursuit eye movements in area MT of macaque monkeys. *Journal of Neuroscience*, 19(6), 2224.
- Lorenceau, J., Shiffrar, M., Wells, N., & Castet, E. (1993). Different motion sensitive units are involved in recovering the direction of moving lines. *Vision Research*, 33(9), 1207–1217.
- Lovejoy, L., Fowler, G., & Krauzlis, R. (2009). Spatial allocation of attention during smooth pursuit eye movements. *Vision Research*, 49(10), 1275–1285.
- Masson, G. S., & Castet, E. (2002). Parallel motion processing for the initiation of short-latency ocular following in humans. *Journal of Neuroscience*, 22(12), 5149.
- Masson, G. S., Proteau, L., & Mestre, D. R. (1995). Effects of stationary and moving textured backgrounds on the visuo-oculo-manual tracking in humans. *Vision Research*, 35(6), 837–852.
- Masson, G. S., & Stone, L. (2002). From following edges to pursuing objects. *Journal of Neurophysiology*, 88(5), 2869.
- Miura, K., Kobayashi, Y., & Kawano, K. (2009). Ocular responses to brief motion of textured backgrounds during smooth pursuit in humans. *Journal of Neurophysiology*, 102(3), 1736.
- Pack, C., Berezovskii, V., & Born, R. (2001). Dynamic properties of neurons in cortical area MT in alert and anaesthetized macaque monkeys. *Nature*, 414(6866), 905–908.
- Pack, C., & Born, R. (2001). Temporal dynamics of a neural solution to the aperture problem in visual area MT of macaque brain. *Nature*, 409(6823), 1040–1042.
- Rashbass, C. (1961). The relationship between saccadic and smooth tracking eye movements. *The Journal of Physiology*, 159(2), 326.

- Recanzone, G., & Wurtz, R. (1999). Shift in smooth pursuit initiation and MT and MST neuronal activity under different stimulus conditions. *Journal of Neurophysiology*, 82(4), 1710.
- Smeets, J., & Bekkering, H. (2000). Prediction of saccadic amplitude during smooth pursuit eye movements. 1. *Human Movement Science*, 19(3), 275–295.
- Smith, M., Majaj, N., & Movshon, J. (2005). Dynamics of motion signaling by neurons in macaque area MT. *Nature Neuroscience*, 8(2), 220–228.
- Spering, M., & Gegenfurtner, K. R. (2007a). Contextual effects on smooth-pursuit eye movements. *Journal of Neurophysiology*, 97(2), 1353.
- Spering, M., & Gegenfurtner, K. R. (2007b). Contrast and assimilation in motion perception and smooth pursuit eye movements. *Journal of Neurophysiology*, 98(3), 1355.
- Spering, M., & Gegenfurtner, K. R. (2008). Contextual effects on motion perception and smooth pursuit eye movements. *Brain Research*, 1225, 76–85.
- Spering, M., Gegenfurtner, K. R., & Kerzel, D. (2006). Distractor interference during smooth pursuit eye movements. *Journal of Experimental Psychology*, 32(5), 1136–1154.
- Tanaka, M., Yoshida, T., & Fukushima, K. (1998). Latency of saccades during smooth-pursuit eye movement in man directional asymmetries. *Experimental Brain Research*, 121(1), 92–98.
- van Donkelaar, P., & Drew, A. (2002). The allocation of attention during smooth pursuit eye movements. *Progress in Brain Research*, 140, 267–277.
- Wallace, J., Stone, L., & Masson, G. S. (2005). Object motion computation for the initiation of smooth pursuit eye movements in humans. *Journal of Neurophysiology*, 93(4), 2279.
- Watamaniuk, S. N. J., & Heinen, S. J. (1999). Human smooth pursuit direction discrimination. *Vision Research*, 39(1), 59–70.
- Watamaniuk, S. N. J., Sekuler, R., & Williams, D. W. (1989). Direction perception in complex dynamic displays: The integration of direction information. *Vision Research*, 29(1), 47–59.
- Wichmann, F., & Hill, N. (2001). The psychometric function: I. Fitting, sampling, and goodness of fit. *Perception and Psychophysics*, 63(8), 1293–1313.
- Yantis, S., & Jonides, J. (1984). Abrupt visual onsets and selective attention: Evidence from visual search. *Journal of Experimental Psychology: Human Perception and Performance*, 10(5), 601–621.